



ACADEMIC  
PRESS

Available online at [www.sciencedirect.com](http://www.sciencedirect.com)

SCIENCE @ DIRECT®

Journal of Solid State Chemistry 173 (2003) 227–231

JOURNAL OF  
SOLID STATE  
CHEMISTRY

<http://elsevier.com/locate/jssc>

# Phase-controlled synthesis and characterization of nickel sulfides nanorods

Guozhen Shen, Di Chen, Kaibin Tang,\* Changhua An, Qing Yang, and Yitai Qian

*Department of Chemistry, Structure Research Laboratory, University of Science and Technology of China, Hefei, Anhui 230026, PR China*

Received 18 July 2002; received in revised form 3 December 2002; accepted 14 December 2002

## Abstract

Different one-dimensional nickel sulfides, NiS nanorods and Ni<sub>9</sub>S<sub>8</sub> nanorods were synthesized in the presence (Route 1) and absence (Route 2) of gas CO<sub>2</sub>. X-ray powder diffraction patterns, scanning electron microscopy and transmission electron microscopy images show that the product from Route 1 is NiS nanorods with a diameter of about 50–120 nm, while the product from Route 2 is Ni<sub>9</sub>S<sub>8</sub> nanorods about 70–200 nm in diameter. A molecular-template-like mechanism was proposed for the one-dimensional structures growth. The products were also investigated by Raman and photoluminescence (PL) spectroscopy.

© 2003 Elsevier Science (USA). All rights reserved.

*Keywords:* Nickel sulfides; Nanorods; Molecular-template-like mechanism; Solvothermal route

## 1. Introduction

Material scientists are attempting to produce novel materials. Development of a controlled-synthesis method is always the most important goal. One-dimensional structures with nanoscale diameters such as nanowires, nanorods, and nanotubes are currently the focus of much attention because of their special properties [1]. Compared to micrometer-diameter whiskers, these fascinating systems are expected to exhibit remarkable mechanical properties, as well as electrical, optical, and magnetical properties that are quite different from those of their corresponding bulk materials [2]. These new nanoscale materials have potential applications in both mesoscopic research and the development of nanodevices. Previous work in this field focused on carbon nanorods and nanotubes, which were the byproducts of fullerene research [3]. Although morphological control has recently been demonstrated [4], synthetic control of nanocrystalline shape remains a daunting task and is a new challenge to scientists.

In recent years, the nickel sulfides and the phase relations in the Ni–S system have been the subject of numerous studies because they can be used as a hydrogenation catalyst, and as a possible transforma-

tion toughener [5–9]. Traditionally, NiS was prepared by solid-state reactions at high temperature and vapor phase reactions [10,11]. Recently, many mild methods have been developed to prepare NiS [12,13]. Jeong et al. synthesized nickel sulfides in aqueous solution [14] and Jiang et al. [15] synthesized NiS layer-rolled structures in aqueous ammonia solution. The solvothermal reaction was also used to prepare NiS nanoparticles [16]. However, as far as we know, the synthesis of one-dimensional NiS nanorods and Ni<sub>9</sub>S<sub>8</sub> nanorods are seldom reported in the literature.

Herein, we report the synthesis of NiS nanorods and Ni<sub>9</sub>S<sub>8</sub> nanorods via a simple solvothermal route using gas CO<sub>2</sub> as the phase controlled additive.

## 2. Experimental

### 2.1. Preparation of NiS nanorods (Route 1)

In a typical procedure, 35 ml hydrazine hydrate was saturated with CO<sub>2</sub> gas, then 0.576 g NiCl<sub>2</sub>·6H<sub>2</sub>O was added to it under continuous stirring until the precipitate was just dissolved. Then slightly excessive Na<sub>2</sub>S<sub>2</sub>O<sub>3</sub> was added into the precursor solution. The mixture was put into a Teflon-lined autoclave of 50 ml capacity. The sealed autoclave was maintained at 165°C

\*Corresponding author. Fax: +86-551-3601600.

E-mail address: [kbtang@ustc.edu.cn](mailto:kbtang@ustc.edu.cn) (K. Tang).

for 20 h and then cooled to room temperature, naturally. Black precipitate was collected by filtration and washed several times with distilled water and absolute ethanol and then vacuum dried at 65°C for 4 h.

## 2.2. Preparation of $\text{Ni}_9\text{S}_8$ nanorods (Route 2)

In this procedure, 0.576 g  $\text{NiCl}_2 \cdot 6\text{H}_2\text{O}$  was dissolved in 35 ml hydrazine hydrate with continuous stirring resulting in a transparent solution. After that, slightly excessive  $\text{Na}_2\text{S}_2\text{O}_3$  was added into the precursor solution. The mixture was put into a Teflon-lined autoclave. The sealed autoclave was also maintained at 165°C for 20 h and then cooled to room temperature, naturally. The obtained product was treated as Route 1.

The samples were characterized by X-ray powder diffraction (XRD). The XRD analysis was carried out on a Japan Rigaku D/max  $\gamma\text{A}$  X-ray diffractometer equipped with a graphite monochromatized  $\text{CuK}\alpha$  radiation ( $\lambda = 1.54178 \text{ \AA}$ ). The samples were scanned at a scanning rate of  $0.05^\circ/\text{s}$  in the  $2\theta$  range of  $10\text{--}70^\circ$ . The microstructure and morphologies of the samples were analyzed with scanning electron microscopy (SEM) and transmission electron microscopy (TEM). SEM images were taken with a KYKY1010B scanning electron microscope (Beijing, China). TEM images were taken with a Hitachi H-800 transmission electron microscope, using an accelerating voltage of 200 kV. The Raman spectra were produced at room temperature with an LABRAM-HR Confocal Laser MicroRaman spectrometer. Photoluminescence (PL) spectra of the samples were measured in a Hitachi 850 fluorescence spectrophotometer with an Xe lamp at room temperature.

## 3. Results and discussion

Fig. 1a displays the XRD pattern of the sample produced from Route 1. All the peaks can be indexed as the hexagonal structure of NiS with lattice parameters  $a = 9.5928 \pm 0.006 \text{ \AA}$ ,  $c = 3.1439 \pm 0.007 \text{ \AA}$ , which is consistent with the reported data ( $a = 9.620 \text{ \AA}$ ,  $c = 3.149 \text{ \AA}$ , JCPDS Card No. 12-0041). No impurities such as Ni,  $\text{NiO}_x$  or intermediary phase nickel sulfides are detected in the XRD pattern. The XRD pattern of the sample from Route 2 (Fig. 1b) exhibits the orthorhombic structure of  $\text{Ni}_9\text{S}_8$  with lattice parameters  $a = 9.3454 \pm 0.008 \text{ \AA}$ ,  $b = 11.2386 \pm 0.028 \text{ \AA}$ ,  $c = 9.3189 \pm 0.010 \text{ \AA}$ , which is consistent with the reported data ( $a = 9.335 \text{ \AA}$ ,  $b = 11.21 \text{ \AA}$ ,  $c = 9.430 \text{ \AA}$ , JCPDS Card. No. 78-1886).

Fig. 2a and b are the SEM images of as-prepared samples. It can be seen that both the products mainly consist of solid rod-like structures.

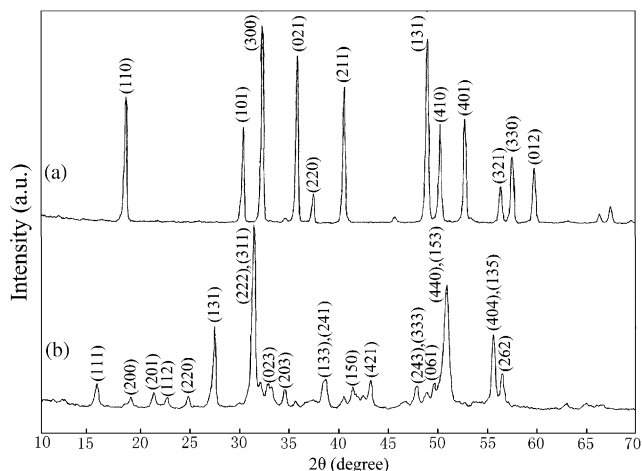


Fig. 1. XRD patterns of the samples. (a) XRD pattern of NiS; and (b) XRD pattern of  $\text{Ni}_9\text{S}_8$ .

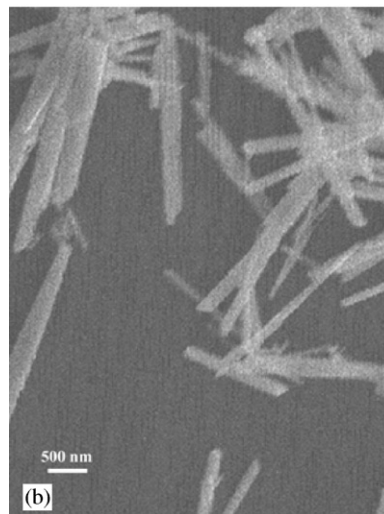
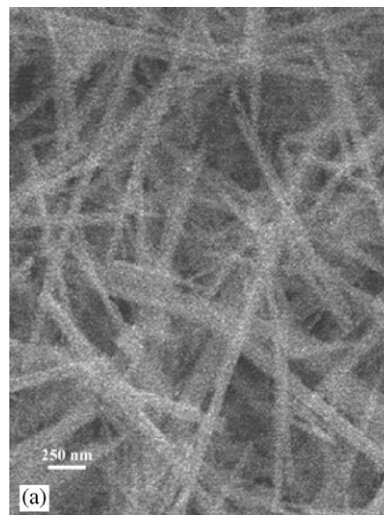


Fig. 2. SEM images of the obtained samples. (a) SEM image of NiS; and (b) SEM image of  $\text{Ni}_9\text{S}_8$ .

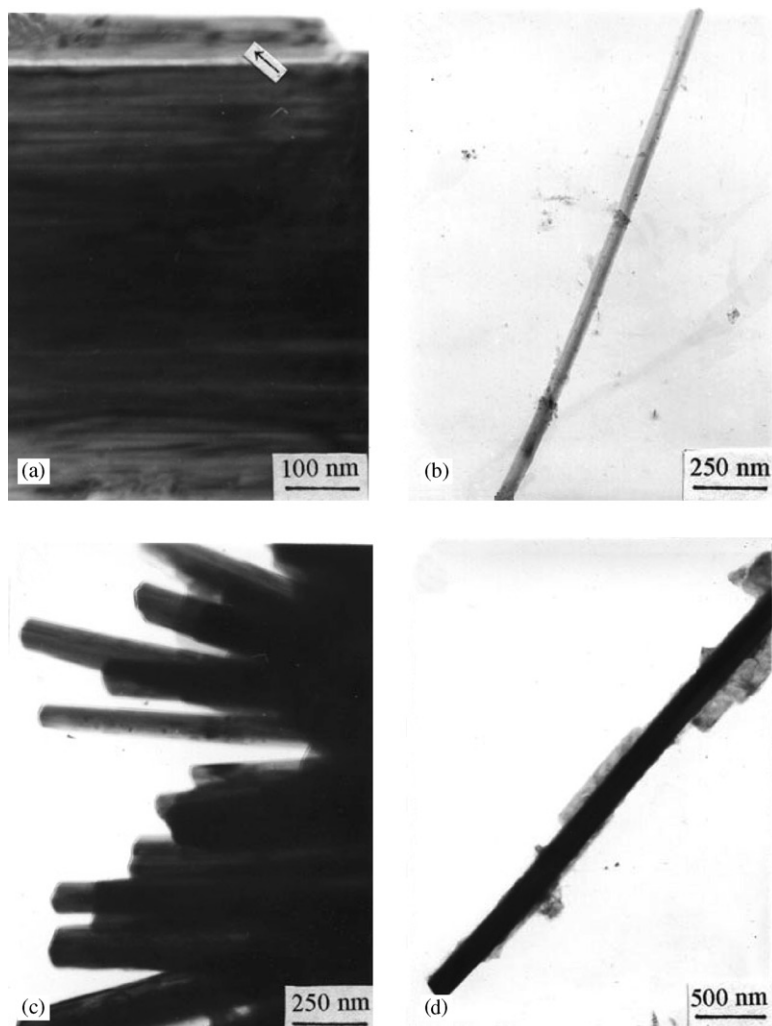


Fig. 3. (a) TEM image of a single NiS nanorods with many aligned nanorods; (b) TEM image of a single NiS nanorod; (c) TEM image of Ni<sub>9</sub>S<sub>8</sub> nanorods; and (d) TEM image of a single Ni<sub>9</sub>S<sub>8</sub> nanorod.

These results can also be proved by TEM procedure. According to the TEM observation of the product from Route 1, lots of nanorods can be observed. Fig. 3a is a TEM image of a single NiS nanorod with some aligned nanorods. From a TEM of a single NiS nanorod (Fig. 3b), one can see that a typical NiS nanorod has a diameter of about 50 nm and length up to 5  $\mu$ m.

As for the sample prepared from Route 2, it can be seen that the product consists mainly of nanorods. From Fig. 3c, the Ni<sub>9</sub>S<sub>8</sub> nanorods produced from the present route typically have diameters of 70–200 nm and lengths up to several micrometers. TEM image of a single nanorod of about 200 nm in diameter was shown in Fig. 3d.

The samples were also characterized by Raman spectra. Fig. 4 shows the Raman spectra for NiS nanorods and Ni<sub>9</sub>S<sub>8</sub> nanorods. The vibrational frequencies derived from the spectra are listed in Table 1. Compared with the reported data, it can be seen that

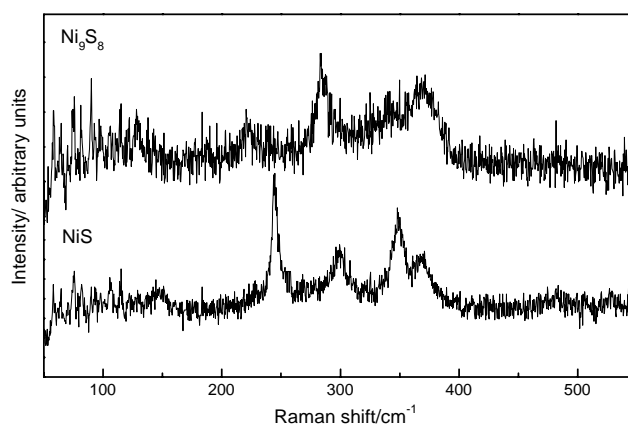


Fig. 4. Room temperature Raman spectra of the obtained samples.

they are in good accordance [18]. For comparison, the data of the literature are also listed in the table.

Fig. 5 shows the PL spectrum from the obtained NiS nanorods at room temperature. In the figure, the

Table 1  
List of the vibrational frequencies ( $\text{cm}^{-1}$ ) derived from the spectra shown in Fig. 4

NiS powders [19] Peak position ( $\Delta \text{cm}^{-1}$ )	$\text{Ni}_9\text{S}_8$ nanorods Peak position ( $\Delta \text{cm}^{-1}$ )	NiS nanorods Peak position ( $\Delta \text{cm}^{-1}$ )
142		144
174		
181		
222	222	
246		244
283	284	
301		300
350	344	349
372	372	369

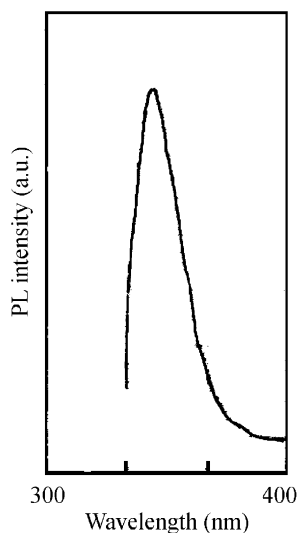
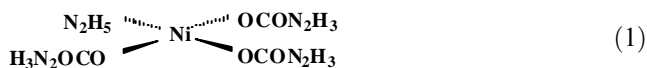


Fig. 5. Photoluminescence spectra for aligned NiS nanorods bundles.

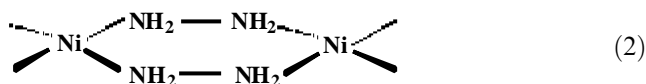
excitation wavelength was 250 nm and the filter wavelength was 310 nm. It is clear that a strong peak centered at 340 nm is observed on the spectrum. From the spectra, no sharp PL lines, which are attributable to impurity-bound excitons and their phono replicas, are clearly seen [15]. The PL spectrum of  $\text{Ni}_9\text{S}_8$  has some similarities with that of NiS and the spectrum was not shown.

Metal hydrazine carboxylates,  $M(\text{N}_2\text{H}_3\text{COO})_2 \cdot 2\text{H}_2\text{O}$  ( $M = \text{Mg, Ca, Mn, Fe, Co, Ni, Cu}$ ), have been used as precursors to fine particle oxide materials [17,19,20]. The novelty of these precursors is due to their low-temperature ( $< 300^\circ\text{C}$ ) autocatalytic exothermic decomposition with the evolution of large amounts of gases to yield fine particles having high surface area oxide. And Dhas extended this method to prepare copper particles [21]. In our synthetic Route 1, when  $\text{NiCl}_2$  was added into the  $\text{CO}_2$  saturated hydrazine hydrate solution, a complex formed in this route, and it can be expressed, according to the above literatures [17], as



This complex is expected to decrease with the increase in temperature. At some relatively high temperature, the newly formed  $\text{S}^{2-}$  anion may coordinate to the complex, producing a one-dimensional NiS nanorod structure to become dense; the bidentate ligands are gradually lost. In the liquid phase, the newly formed  $\text{S}^{2-}$  attacks the complex, which causes the bonds between  $\text{Ni}^{2+}$  and the ligands to become weaker and the bonds between the  $\text{Ni}^{2+}$  and  $\text{S}^{2-}$  to form gradually. And finally,  $\text{Ni}^{2+}$  and the ligands separate from each other.  $\text{Ni}^{2+}$  are connected by  $\text{S}^{2-}$ , and in the end they form a one-dimensional NiS nanorods structure.

In Route 2, the formation of rod-like  $\text{Ni}_9\text{S}_8$  crystals indicated that the nucleation and growth were well controlled. Solvent hydrazine hydrate plays an important role in the growth of as-prepared  $\text{Ni}_9\text{S}_8$  nanorods. Since hydrazine hydrate is a bidentate ligand, it can react with metal ion to form a relatively stable metal complex [22–24]. In the reaction, when  $\text{NiCl}_2$  is added into hydrazine hydrate solution, a transparent solution is formed. So it is reasonable to think that  $\text{Ni}^{2+}$  complex (2) depicted below is formed:



The stability of the complexes is expected to decrease with the increase in temperature. At some relatively high temperature, for example, above  $160^\circ\text{C}$ , the  $\text{S}^{2-}$  anion from  $\text{S}_2\text{O}_3^{2-}$  may coordinate to the above complex to form a one-dimensional  $\text{Ni}_9\text{S}_8$  nanorod structure and the volatile coordinated ligands are lost gradually. The detailed growth mechanism may have a number of similarities with the formation of one-dimensional NiS nanorods.

Based on the above mechanism analyses, it can be concluded that the growth of as-prepared samples has a similar growth mechanism. In the process of  $\text{Ni}_9\text{S}_8$  nanorods and NiS nanorods formation, both the mentioned complexes ((1) and (2)) could serve as a molecular template in control of the one-dimensional structures growth.

In order to improve our understanding of the template effect, we replaced hydrazine with benzene, toluene, and  $\text{CCl}_4$ , which have no coordination ability, and keeping the other reaction condition constant, only NiS nanoparticles or no NiS could be obtained. With regard to the pyridine, which has a relatively weak N-coordinating ability but a lack of bidentate coordinate, TEM observations show that only a small fraction of nanorods was obtained. So we speculate these nanorods growth mechanism as a molecular-template-like mechanism.

In our experiments, it was found that using  $\text{Na}_2\text{S}_2\text{O}_3$  as the sulfur source is also an important factor for the formation of one-dimensional structures. Using other sulfur sources, such as thiourea,  $\text{Na}_2\text{S}$ , only nickel

sulfides nanoparticles could be obtained under the same conditions.

#### 4. Conclusion

In summary, one-dimensional structures of NiS and Ni<sub>9</sub>S<sub>8</sub> were successfully synthesized through a simple solvothermal route in the presence and absence of gas CO<sub>2</sub>. Studies found that addition of gas CO<sub>2</sub> and use of Na<sub>2</sub>S<sub>2</sub>O<sub>3</sub> are the key factors for the formation of one-dimensional structures. Based on the experiments, a molecular-template-like growth mechanism was proposed. Although the molecular-template-like mechanism was proposed for the one-dimensional structures growth, the detailed growth mechanism still needs to be investigated.

#### Acknowledgments

This work was supported by Chinese National Natural Science Research Foundation and the 973 Projects of China.

#### References

- [1] A.M. Rao, E. Richter, S. Bandow, B. Shase, P.C. Eklund, L.A. Williams, S. Fang, K.R. Subbaswamy, M. Menon, A. Thess, R.E. Smalley, G. Dresselhaus, M.S. Dresselhaus, *Science* 275 (1997) 187.
- [2] A.P. Alivisatos, *Science* 271 (1996) 933.
- [3] S. Iijima, *Nature* 354 (1991) 56.
- [4] N. Herron, J.C. Calabrese, W.E. Farnet, Y. Wang, *Science* 259 (1995) 1426.
- [5] K.M. Abraham, J.E. Elliot, *J. Electrochem. Soc.* 131 (1984) 2211.
- [6] O. Weisser, S. Landa, *Sulfide Catalysts, Their Properties and Applications*, Pergamon, Oxford, 1973, pp. 167, 171.
- [7] H. Vandenberg, Ph. Vermeiren, R. Leysen, *Electrochim. Acta* 29 (1984) 297.
- [8] W.M. Kriven, *J. Am. Ceram. Soc.* 71 (1988) 1021.
- [9] A. Olivas, J. Cruz-Reyes, V. Petranovskii, M. Avalos, S. Fuentes, *J. Vac. Sci. Technol. A* 16 (1998) 3515.
- [10] R. Coustal, *J. Chem. Phys.* 38 (1958) 277.
- [11] D. Delafosse, P. Barret, *C. R. Acad. Sci.* 252 (1961) 888.
- [12] G. Henshaw, I.P. Parkin, G.A. Shaw, *J. Chem. Soc. Dalton Trans.* 2 (1997) 231.
- [13] B.O. Dusastre, I.P. Parkin, G.A. Shaw, *J. Chem. Soc. Dalton Trans.* 19 (1997) 3503.
- [14] Y.U. Jeong, A. Manthiram, *Inorg. Chem.* 40 (2001) 73.
- [15] X.C. Jiang, Y. Xie, J. Lu, L.Y. Zhu, W. He, Y.T. Qian, *Adv. Mater.* 13 (2001) 1278.
- [16] Z.Y. Meng, Y.Y. Peng, L.Q. Xu, Y.T. Qian, *Mater. Lett.* 53 (2002) 165.
- [17] S.S. Manoharan, K.C. Patil, *Proc. Ind. Acad. Sci.* 101 (1989) 377.
- [18] D.W. Bishop, P.S. Thomas, A.S. Ray, *Mater. Res. Bull.* 33 (1998) 1303.
- [19] D. Ravindranathan, K.C. Patil, *Ceram. Bull.* 66 (1987) 688.
- [20] D. Ravindranathan, K.C. Patil, *J. Mater. Sci.* 22 (1987) 3261.
- [21] N.A. Dhas, C.P. Raj, A. Gedanken, *Chem. Mater.* 10 (1998) 1446.
- [22] F.A. Cotton, G. Wilkinson, *Advanced Inorganic Chemistry*, 3rd Edition, Wiley, New York, 1972.
- [23] Y.F. Liu, J.H. Zeng, W.X. Zhang, W.C. Yu, Y.T. Qian, J.B. Cao, W.Q. Zhang, *J. Mater. Res.* 16 (2001) 3361.
- [24] K. Matsumoto, H. Uemura, M. Kawano, *Chem. Lett.* 7 (1994) 1215.